

Comparing active Gilbert mixers integrated in standard SiGe process (Part I)

Up until now, mixers from different fabrication processes have been compared. But with the fabrication process affecting performance, different mixers resulting from the standard SiGe process should be compared.

By N. Rodríguez, E. Hernández, G. Bistué, I. Gutiérrez, J. Presa and R. Berenguer

Several design options exist for active Gilbert mixers that are integrated in the standard 0.8 μm SiGe process. The first design option is to optimize the noise figure obtaining the lowest noise for a specific fabrication process: a mixer with 9.7 dB NF, 13.5 dB gain and -5 dBm iIP3 is presented as a reference for the other designs. The second option is to modify Gilbert cells to improve linearity. However, this implies gain reduction.

Two methods increase linearity including emitter degeneration or changing the RF input stage. With the first method, the iIP3 value becomes 12.4 dB, which is 17.4 dB higher than the previous one, but voltage gain is 10.7 dB lower. The second uses class AB as the bi-symmetrical RF input stage. The iIP3 is 7.2 dB, and the rise is only 12.2 dB. But voltage gain is only reduced by 3.8 dB. The comparison between mixer measurements gives us the improvement range that can be obtained by the sole design approach and by avoiding technological influence.

In a digital receiver, the components from the output of the antenna to the input of the analog to digital converter (ADC), is considered the RF front end. In this chain of RF components, the mixer is one of the key elements because it provides the necessary frequency downconversion that makes the receiver capable of processing the incoming signal.

The mixer performance has a great influence on the characteristics of the overall front end. Since it follows the low-noise amplifier (LNA), the issue of linearity becomes significant because it must handle amplified signals. While it may seem that the issue of noise is relaxed by the LNA gain, in practice, mixers exhibit a high noise figure that should also be taken into account. The gain of the mixer is also important to compensate for the intermediate frequency (IF) filter loss and to reduce the noise contribution from the IF stages. So in the design of a mixer, it is always necessary to achieve a trade-off among the three main parameters: gain, noise figure and linearity.

When designing a Gilbert cell to fulfill some specific requirements, the first step is to compare the performance of different mixers reported in the bibliography.^[1,2,3] However their fabrication processes, even though they were named with the same common noun, include differences such as substrate characteristics or base doping density of the heterobipolar transistor (HBT). These are decisive factors in mixer performance. For this reason, differences between mixers designed by different authors are a combination of changes in mixer structure and in technology process.

The objective of this paper is to provide an idea of the improve-

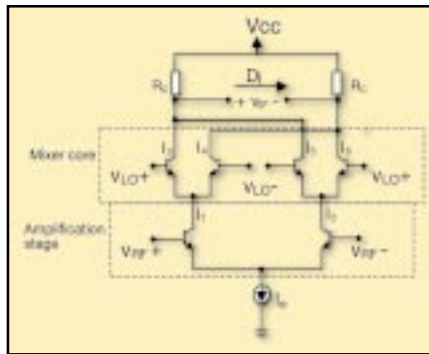


Figure 1. Gilbert cell. (V_{LO} : local oscillator voltage input signal; V_{RF} : RF voltage input signal; R_C : collector resistance; V_{CC} : voltage supply; V_{IF} : intermediate frequency voltage output signal; I_e : bias current).

ment that can be obtained in the conversion gain, noise figure and linearity of Gilbert cells. The first stage is to explain the design guidelines of Gilbert cells that are used to optimize mixers. To guarantee that the design guidelines only depend on mixer structure and not on the fabrication process, all the mixers here have been designed with the same process, a standard 0.8 μm SiGe.

Design guidelines

Here, the main design guidelines of Gilbert cells are detailed.^[4] Gilbert mixers are the most widely used active mixers. This mixer is formed by two stages: the amplification stage and the mixing core (Figure 1).

In the following subsections, the mixer performance is expressed as a function of some individual components (collector resistance R_C , transistor size, number of base contacts, bias current of the mixer I_e). Mixer design guidelines are extracted from the behavioral mathematical model equations and from the authors' previous experience in mixer design.

Conversion gain in Gilbert mixers—The conversion gain value is obtained by multiplying two voltage signals: the well-known output voltage (V_{od}) of the input differential pair.^[5] (Eq. 1):

$$V_{od} = \alpha_F I_e R_C \tanh\left(\frac{V_{RF}^- - V_{RF}^+}{2V_T}\right) = 2I_C R_C \tanh\left(\frac{-V_{RF}}{2V_T}\right),$$

where I_C is the collector current, V_{RF} is the input voltage, and V_T is the thermal voltage. In Equation 1, when RF is a small signal, the hyperbolic tangent of x can be approximated by x , therefore, (Eq. 2):

$$V_{od} = 2I_C R_C \left(\frac{-V_{RF}}{2V_T}\right)$$

On the other hand, when having a square local oscillator (LO) signal, it can be approximated by the first term of a Taylor series (Eq. 3):

$$V_{LO} = \frac{2}{\pi}$$

The voltage gain can be obtained by multiplying Equations 2 and 3. When LO switches are driving current, the collector resistor for the amplification stage is R_C and r_E of transistors in amplification stage. Normally $r_E \ll R_C$. But r_E is not included in equation (Eq. 4):

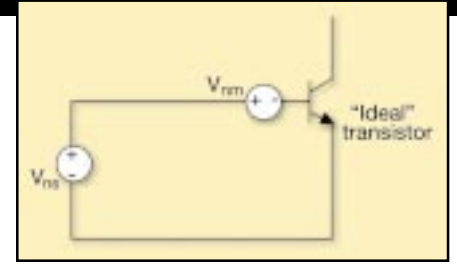
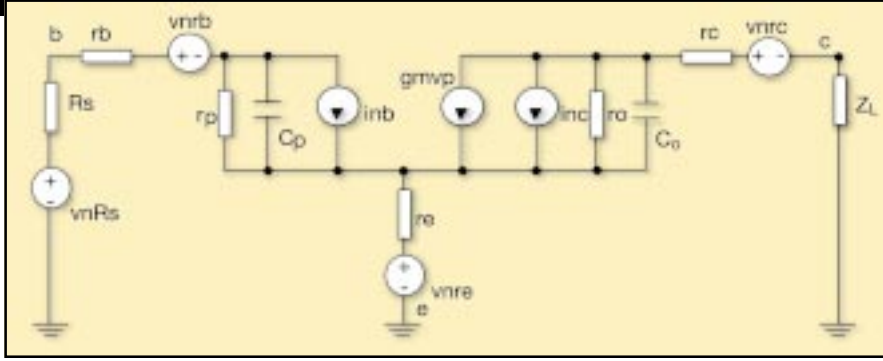


Figure 3: Noise model of transistor

Figure 2. Hybrid- π noise model.

$$\frac{V_{IF}}{V_{RF}} = G_v = -R_C g_{mRF} \frac{2}{\pi},$$

where G_v is the voltage conversion gain, R_C the collector resistance and g_{mRF} is the transconductance of the transistors in the amplification stage. As can be seen from Equation 4, to increase gain:

1. The transconductance of transistors in amplification stage g_{mRF} should be as high as possible. This parameter is directly influenced by bias current I_e .
2. Collector resistance R_C should be as big as possible. The limit of this resistor value depends on the output frequency because of the gain-bandwidth trade-off.

Noise figure in Gilbert mixers—The main contributor to noise figure in Gilbert mixers is the amplification stage because afterward the signal has already been amplified. Also, applying Friis equation^[7], the noise added to signal after amplification has less importance. To obtain an idea about the amount of noise added in this stage, each transistor in the differential pair is substituted for its quasi-linear noise model^[9] that can be used at frequencies below 6 GHz.

Resistances (R_s , r_b , r_e and r_c) generates thermal noise as can be seen in (Eq. 5):

$$v_{nr}^2 = 4kTr,$$

where k is the Boltzmann's constant, T is temperature and r is the resistance value (Ω).

Base and collector currents (I_b and I_c) generate shot noise (Eq. 6):

$$i_{nb}^2 = \frac{2KTg_m}{\beta}$$

$$i_{nc}^2 = 2kTg_m,$$

where g_m is the HBT transconductance.

Base current (I_b) also generates flicker noise (Eq. 7):

$$i_{nf}^2 = \frac{2q I_b f_1}{f},$$

where f_1 is the corner frequency and f is the frequency of interest. The flicker noise defined by Equation 7 becomes dominant at lower frequencies, below the corner, f_1 value and can be neglected above a few kHz.

Three noise generators must be added: two current sources that represent the shot noise of the collector and base currents and four voltage sources that represent the noise generated by the source resistance (R_s), parasitic base, emitter and collector resistances, r_b , r_e and r_c . Transferring all these sources to the input yields noise generated at source and the mixer, as shown in Figure 3.

The term V_{ns} is the noise generated in the source, and V_{nm} is the noise of the mixer converted to a voltage source at the input. The different noise sources included in V_{nm} are (Eq. 8):

$$v_{nm}^2 = v_{nr}^2 + v_{nb}^2 + v_{nc}^2,$$

where V_{nr} is the thermal noise of parasitic resistances, V_{nb} is the base-emitter shot noise and V_{nc} is the collector-emitter shot noise.

Thermal noise of parasitic base and emitter resistances are shown in (Eq. 9):

$$v_{nr}^2 = 4kT(r_b + r_e).$$

The thermal noise of collector resistor is disregarded because the noise of r_c is typically 105 times lower than collector emitter shot noise [9].

Base-emitter shot noise is converted to voltage noise source in series with the source resistor applying Thevenin conversion (Eq. 10):

$$v_{nb}^2 = \frac{2KTg_m(r_b + r_e + Z_n)^2}{\beta}$$

where Z_n is the base impedance.

The voltage source associated to the collector-emitter shot noise is (Eq. 11):

$$v_{nc}^2 = \frac{2KT}{g_m} \left(1 + \frac{(r_b + r_e + Z_n)^2}{Z_{be}^2} \right),$$

where Z_{be} is the parallel of r_π and c_π in Figure 2.

The noise figure expression of a device can be obtained from the ratio between the total noise at the output and the noise of the source (Eq. 12):

$$F = \frac{Gv_{ns}^2 + Gv_{nm}^2}{Gv_{ns}^2} = \frac{v_{ns}^2 + v_{nm}^2}{v_{ns}^2} = 1 + \frac{v_{nm}^2}{v_{ns}^2},$$

where v_{ns} is the noise at the input of the device and v_{nm} is the noise of the device.

By substituting Equations 7, 8 and 9 in 10, the noise figure expression is obtained (Eq. 13):

$$F = 1 + \frac{r_b + r_e}{\text{Re}(Z_n(t))} + \frac{1}{2g_m(t)\text{Re}(Z_n(t))} + \frac{g_m(t)(r_b + r_e + Z_n(t))^2}{2\beta \text{Re}(Z_n(t))} + \frac{(r_b + r_e + Z_n(t))^2}{2g_m(t)\text{Re}(Z_n(t))\text{Re}(Z_{be})^2},$$

where g_m and Z_n are time-dependent variables because in the previous calculus the first stage of the mixer has been modeled using a small signal model of the transistor. As the mixer is not a linear device, g_m and Z_n are not constant values. In [9] a model to predict noise figure of HBT mixer is presented by splitting the influence of LO harmonics in noise figure (Eq. 14):

$$F = 1 + \frac{r_b + r_e}{\text{Re}(Z_{-1})} + \frac{(r_b + r_e + Z_{-1})^2}{2\beta \text{Re}(Z_{-1})} g_{-1} + \frac{1}{2g_1 \text{Re}(Z_{-1})} + \frac{(r_b + r_e + Z_{-1})^2}{2\text{Re}(Z_{-1})r_\pi^2} \frac{1}{g_1}$$

$$+ \frac{Y_0}{Y_1 \text{Re}(Z_{-1})} \left[(r_b + r_e + \text{Re}(Z_0)) + \frac{(r_b + r_e + Z_0)^2}{2\beta} g_0 + \frac{1}{2g_0} + \frac{(r_b + r_e + Z_0)^2}{2R_\pi^2} \frac{1}{g_0} \right]$$

$$+ \frac{Y_{-1}}{Y_1 \text{Re}(Z_{-1})} \left[(r_b + r_e + \text{Re}(Z_1)) + \frac{(r_b + r_e + Z_1)^2}{2\beta} g_1 + \frac{1}{2g_{-1}} + \frac{(r_b + r_e + Z_1)^2}{2R_\pi^2} \frac{1}{g_{-1}} \right],$$

where the rows of Equation 14 are the noise contribution from RF, direct current (DC) and image frequencies to IF output, respectively. The three rows have a similar structure: Thermal noise form resistances, base shot noise contribution and the elements multiplied by $(1/g_i)$ are the collector shot noise contribution.

Influence of Mixer Design in Noise Figure—Analyzing Equation 14 to minimize noise figure of the mixers shows two main parameters that influence the noise figure of the differential pair and that must be taken into account when designing a mixer. The base and emitter resistances r_b and r_e are the only parameters of the transistors that affect thermal noise and can be modified by the designer. To reduce the noise generated by r_b and r_e , the number of base-emitter contacts and the emitter area must be as high as possible. However, there are limits to the possible emitter area because of the parasitic capacitance c_π which is proportional to the emitter area. This capacitance affects the impedance Z in Equation 14. So, depending on the RF, a trade-off must be achieved between reducing thermal noise and reducing gain that induces a rise in noise figure due to the higher influence of noise from next stages. The transconductance g_m is directly proportional to the collector current I_C , and this current is fixed when polarizing the mixer. If the transistor parameter β is high, the base shot noise contribution can be neglected and I_C should be increased. However if β , which depends on frequency, in Equation 13 is not quite high, then shot noise of I_b influences noise figure and I_C should be reduced. The high-frequency small signal current gain [8] is (Eq. 15):

$$\beta(j\omega) = \frac{\beta_0}{1 + \beta_0 \frac{C_\pi + C_\mu}{g_m} j\omega},$$

where C_π is the base-emitter parasitic capacitance and C_μ is the base-collector parasitic capacitance, β_0 is the low frequency current gain and g_m the transconductance of the transistor.

From Equation 14 another consideration can be made: The noise contribution of the second and third row can be minimized by filtering the image and IF.

Once the mixer has been fabricated, there is a way to influence the noise figure as can be seen in Equation 14. LO signal has great influence on noise figure first of all because g_m is directly proportional to LO power. In addition, LO signal has another influence on mixer noise: If switching of the four transistors in mixer core had been ideal (Figure 1), then only two transistors have been conducting in every single moment and only two transistors would have been generating noise. However, there are small intervals when the four transistors are switched on. The length of this interval depends on the LO signal, its voltage level and shape.

Linearity in Gilbert mixers—Gilbert mixer linearity depends mainly on the first stage, which transforms the voltage input signal in a balanced current. This function is carried out by the differential input pair that forms the amplification stage. Its behavior can be defined with an hyperbolic tangent function presented in Equation 1

that is also included in Equation 16 (Eq. 16):

$$V_{od} = 2I_C R_C \tanh\left(\frac{-V_{RF}}{2V_T}\right)$$

In the conversion gain section, Equation 4, a linear conversion has been considered by equating $\tanh(x)$ with x , assuming that the input signal is a small signal. However, when analyzing the mixer linearity, this assumption cannot be made because high input signals are used to test the mixer.

To obtain the different output harmonics the $\tanh(x)$ function is approximated by its Taylor series (Eq. 17):

$$\tanh(x) = \alpha_1 x - \alpha_3 x^3 + \dots$$

If the input signal of the mixer is a two-tone signal (Eq. 18):

$$x(t) = A \cos \omega_1 t + A \cos \omega_2 t,$$

where ω_1 is close to ω_2 frequency and A is the signal amplitude, the output signal is obtained by substituting Equation 17 in Equation 16 (Eq. 19):

$$\begin{aligned} \tanh(x) = & \left(\alpha_1 + \frac{9}{4} \alpha_3 A^2 \right) A \cos \omega_1 t + \left(\alpha_1 + \frac{9}{4} \alpha_3 A^2 \right) A \cos \omega_2 t \\ & + \frac{3}{4} \alpha_3 A^3 \cos(2\omega_1 - \omega_2)t + \frac{3}{4} \alpha_3 A^3 \cos(2\omega_2 - \omega_1)t + \dots \end{aligned}$$

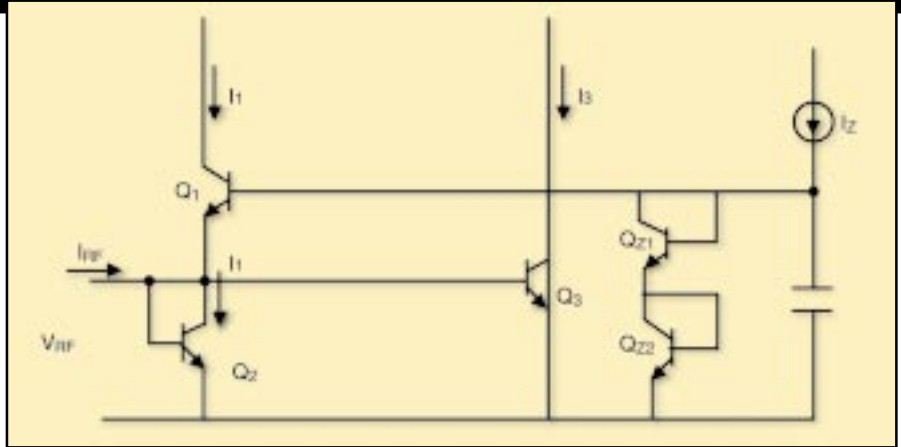


Figure 4. Simplified class-AB input stage.

Linearity is measured through the IP3 parameter, which is the theoretical point where output components at ω_1 and ω_2 have the same amplitudes, as those at $2\omega_1 - \omega_2$ and $2\omega_2 - \omega_1$. If the input amplitude A is small enough to guarantee that $\alpha_1 \gg 9\alpha_3 A^2/4$ ^[10], then the IP3 point is given by (Eq. 20):

$$|\alpha_1| A_{IP3} = \frac{3}{4} |\alpha_3| A_{IP3}^3,$$

where A_{IP3} is the normalized input signal amplitude at IP3 point (Eq. 21):

$$A_{IP3} = \sqrt{\frac{4}{3} \frac{|\alpha_1|}{|\alpha_3|}}$$

and the output IP3 is given by $\alpha_1 A_{IP3}$.

In the input stage of a Gilbert cell, which is a differential pair, the α_1 and α_3 coefficients can be approximated by $\alpha_1=1$ and $\alpha_3=1/3$ for $-0.55 < x < 0.55$ [11]. As $x=V_{RF}/2V_T$, this means inputs up to ± 28.6 mV for a bipolar differential pair operating at $T=300$ K. If the input signal amplitude is the maximum signal, 28.6 mV, which corresponds to -11.84 dBm, then the maximum input IP3 is (Eq. 22):

$$IP3 = 20 \log A_{IP3} + P_{LN} = 20 \log \left(\sqrt{\frac{4}{3}} \frac{|\alpha_1|}{|\alpha_3|} \right) + P_{IN} = -5.82 \text{ dBm}$$

As can be seen in previous equations, Gilbert cell linearity can be approximated by a mathematical function that is not dependent on the values of the elements that form the circuit. Theoretically, the HBT pair in the amplification stage has a linearity limit near -5 dBm. This is the maximum IP3 value obtained in a Gilbert cell, but it can become lower if the layout of the circuit is not carefully designed or a perfect switching is not achieved. To obtain the maximum IP3 value:

1. The switches in the mixer core should be made of small transistors. In this way base-emitter capacitance of switches might be reduced and the transition time decreased. Linearity is improved because the third-order intermodulation currents are only generated in transitions [12].
2. Layout techniques like common centroid should be used to achieve equal branches in Gilbert cell.
3. LO signal in the mixer core (Figure 1) has great influence on linearity. It must drive enough power to switch transistors quickly with the minimum transition time. However, too much power charges

the Cbe parasitic capacitor of transistors in the mixer core and produces current peaks [13].

Local oscillator isolation—Local oscillator isolation depends on differential structure, and isolation is increased by assuring symmetry between the two sides of differential Gilbert cell.

Linearizing techniques

The only way to increase linearity is by modifying Equation 17. Two methods are widely used to linearize Gilbert cells: the inclusion of emitter degeneration [5] and the use of a class-AB input stage, replacing the HBT pair in the amplification stage [11].

Emitter degeneration consists of including emitter resistors in the transistor pair of the RF stage. This is a popular way to extend the linear range of operation. The improvement factor in the differential pair is approximately equal to $I_e R_e$, with I_e and R_e the emitter current and the resistor value, respectively. However, the use of emitter degeneration to improve linearity involves some consequences in gain and noise.

Voltage gain is reduced by approximately the same factor that the input range is increased. Also, a new factor is added in the voltage noise defined by Equation 9 (Eq. 23):

$$V_{nRe}^2 = 4kTR_e,$$

which is the thermal noise resulting from emitter degeneration. In addition, because of voltage gain reduction in differential input stage, the contributions to noise of the following stages become more important.

Two kinds of degeneration can be included in the emitter: resistive or inductive. The resistive is used when the RF signal is a low frequency or a wideband signal and it includes more gain decrease

than the latter one. The inductive degeneration is used with high frequency and narrowband signals.

The bisymmetric class-AB topology based on translinear principles is a linearizing technique that has no inherent gain compression^[14]. The input stage diagram is shown in Figure 4.

In this input stage, the relationship between I_{RF} and the difference between I_1 and I_3 is (Eq. 24):

$$I_{RF} = (I_1 - I_3)$$

so the operation is linear, provided that the input signal is a current.

This stage has several points that must be taken into account when designing a mixer. The input resistance of this stage is (Eq. 25):

$$R_{IN} = \frac{V_T}{2I_1}$$

From Equation 25, it can be seen that, to obtain a 50 W input resistance, a low value of I_1 should be used. However, this current value would result in a poor gain and consequently a higher noise.

Mixer gain associated with this input stage is (Eq. 26):

$$G_V = R_C g_{mRF} \frac{4}{\pi}$$

Comparing Equation 26 with the gain of the differential pair (Equation 4), it can be seen that the gain in mixers employing class AB as input stage is twice the gain obtained in mixers with differential pair in input stage. However, in class AB, the collector current I_c is lower in to achieve the 50 W matching, and for this reason, g_{mRF} is lower. The equation for noise figure in mixers that use class AB as the input stage is quite similar to the noise figure in mixers with Gilbert cells. But it includes some differences. Three transistors are in the input stage, so there are three noisy current sources associated with shot noise from I_c and I_b . The voltage gain is not high enough and the noise from the mixer core and the buffer influences the global noise figure of the mixer. The only way to increase linearity is to modify Equation 17. Two methods are widely used to linearize Gilbert cells: the inclusion of emitter degeneration [5] and the use of class-AB stage (Figure 4), replacing the HBT pair in the amplification stage [11]. RFD

Part II of this article coming next month, will examine and summarize the different design guidelines and will present the measured performance of each design.

References

1. O. Sahana'a, I. Linscott, L. Tyler, "Frequency-Scalable SiGe Bipolar RF Front-End Design," IEEE Journal of Solid State Circuits, vol. 36, N6, pp. 888-895, June 2001.
2. H-D. Wolmuth, W. Simbürger, "A High-IP3 RF Receiver Chip Set for Mobile Radio Base Stations up to 2 GHz," IEEE Journal of Solid State Circuits, vol. 36, N7, pp. 1132-1137, July 2001.
3. J. Rynänen, K. Kivekäs, "A Dual-Band RF Front-End for WCDM and GSM Applications," IEEE Journal of Solid State Circuits, vol. 36, N8, August 2001.
4. B. Gilbert, "A Precise Four-Quadrant Multiplier with Subnanosecond Response," IEEE Journal of Solid State Circuits, vol. SC-3, N4, pp. 365-373, December 1968.
5. P. Gray, R Meyer, "Analysis and Design of Analog Integrated Circuits," Wiley, 1984 (2nd ed.), p. 197.
6. K.L. Fong, "Design and Optimization Techniques for Monolithic RF Downconversion Mixers," Dissertation for the Degree of Doctor of Philosophy, Berkeley, p. 50, 1997.
7. T. H. Lee, "The Design of CMOS Radio-Frequency Integrated Circuits," Cambridge University Press, pp. 552-554, 1998.
8. P. Gray, R. Meyer, "Analysis and Design of Analog Integrated Circuits," Wiley, 1984 (2nd ed.), p. 43.
9. B. Xavier, "Noise Figure & Associated Conversion Gain of a GaAs HBT Mixer," WFC: Interconnects and Packaging for RF Wireless Communications Systems. Tutorial Working Forum, June 1997 (IEEE MTT-S International Microwave Symposium).
10. B. Razavi, "RF Microelectronics," Ed. Prentice Hall 1998, pp. 17-22.
11. B. Gilbert, "Design Considerations for BJT Active Mixers," Analog Devices Inc. 2000.
12. S.A. Maas, "Two-Tone Intermodulation in Diode Mixers," IEEE Transaction on Microwave Theory and Techniques, pp. 307-314, March 1987.
13. T. H. Lee, "The Design of CMOS Radio-Frequency Integrated Circuits," Cambridge University Press, 1998, p. 324.
14. B. Gilbert, "The Micromixer: A Highly Linear Variant of the Gilbert Mixer Using a Bisymmetric Class-AB Input Stage," IEEE Journal of Solid State Circuits, vol. 32, N9, pp. 1412-1423, September 1997.
15. B. Razavi, "A 1.5V 900 MHz Downconversion Mixer," ISSC96, Communications Building Blocks/Paper TP 3.1 pp. 48-49, February 1999.

ABOUT THE AUTHORS

N. Rodríguez, Ph. D. is a telecommunications engineer for the Centro de Estudios e Investigaciones Técnicas de Gipuzkoa (CEIT), San Sebastián, Spain. He can be reached via e-mail at nrodriguez@ceit.es.

E. Hernández, G. Bistué, J. Presa and R. Berenguer are also with CEIT. Bistué is an IEEE member.

I. Gutiérrez is with Tecnun, Escuela Superior de Ingenieros de San Sebastián (Universidad de Navarra), San Sebastián, Spain.

www.rfdesign.com